Clinical and Genetic Characteristics of Chinese Patients with Occult Macular Dystrophy

Dan-Dan Wang,[1–3] Feng-Juan Gao,[1–3] Jian-Kang Li,[4] Fang Chen,[4] Fang-Yuan Hu,[1–3] Ge-Zhi Xu,[1–3] Jian-Guo Zhang,[4] Hao-Xiang Sun,[5] Sheng-Hai Zhang,[1–3] Ping Xu,[1–3] Guo-Hong Tian,[1–3] and Ji-Hong Wu[1–3]

[1]Eye and ENT Hospital, Shanghai Medical College, Fudan University, Shanghai, China
[2]Shanghai Key Laboratory of Visual Impairment and Restoration, Science and Technology Commission of Shanghai Municipality, Shanghai, China
[3]Key Laboratory of Myopia, Ministry of Health, Shanghai, China
[4]BGI-Shenzhen, Shenzhen, China
[5]Sonoma Academy, California, USA

Correspondence: Ji-Hong Wu, Eye and ENT Hospital of Fudan University, 83 Fengyang Road, Shanghai, 200031, China; jihongwu@fudan.edu.cn.
Guo-Hong Tian, Eye, Ear, Nose and Throat Hospital of Fudan University, 83 Fengyang Road, Shanghai 200031, China; valentian99@hotmail.com.

D-DW and F-JG contributed equally to this work.

Received: September 27, 2019
Accepted: December 19, 2019
Published: March 16, 2020

Citation: Wang D-D, Gao F-J, Li J-K, et al. Clinical and genetic characteristics of Chinese patients with occult macular dystrophy. *Invest Ophthalmol Vis Sci.* 2020;61(3):10. https://doi.org/10.1167/iovs.61.3.10

Purpose. To investigate the clinical and genetic characteristics of occult macular dystrophy (OMD) based on a Chinese patient cohort.

Methods. Fifteen Chinese OMD patients from nine unrelated families underwent genetic testing, and all of them harbored a pathogenic *RP1L1* variant. Comprehensive ophthalmic examinations were performed in nine probands, including spectral-domain optical coherence tomography (SD-OCT), near-infrared reflectance (NIR), fundus autofluorescence (AF), and multifocal electroretinography.

Results. The *RP1L1* variants p.R45W and p.S1199C were identified in 13 patients and two patients, respectively, and one was a de novo mutation. Among the nine probands, the median ages at onset and examination were 25.0 years (range, 6–51 years) and 27.0 years (range, 14–55 years), respectively. The median decimal visual acuity was 0.20 (range, 0.04–0.5). Foveal photoreceptor thickness and visual acuity showed a significant correlation ($r = 0.591$; $P = 0.01$). All eyes presented with an absent interdigitation zone and blurred ellipsoid zone of photoreceptors when examined by SD-OCT. In addition, central round lesions with low NIR reflectance were observed in 66.7% (12/18) of eyes by NIR reflectance imaging, corresponding to the regions with abnormal photoreceptor microstructures observed by SD-OCT. Of the 18 eyes, only four eyes showed ring-like faint hyperfluorescence around the macula by AF.

Conclusions. To the best of our knowledge, this is the largest study in a cohort of Chinese OMD patients with *RP1L1* mutations. Our findings revealed that the two recurrent *RP1L1* variants are related to OMD in the Chinese population. Furthermore, multimodal imaging combined with genetic testing is valuable for diagnosing and monitoring OMD progression.

Keywords: occult macular dystrophy, *RP1L1*, multimodal imaging, next-generation sequencing, early diagnostics

Occult macular dystrophy (OMD, OMIM 613587) is a hereditary macular dystrophy that was first described by Miyake et al. in 1989.[1] Patients present with bilateral or sequential progressive visual decline. The characteristic clinical finding is reduced amplitudes on focal macular electroretinography (ERG) or multifocal ERG (mfERG) tests,[2] whereas full-field ERG (ffERG) results, fluorescein angiogram (FA) results, and fundus appearance are usually normal. In addition, spectral-domain optical coherence tomography (SD-OCT) shows the absence of the interdigitation zone (IZ) and blurring of the ellipsoid zone (EZ) of photoreceptors at the macula.[3,4]

Retinitis pigmentosa 1-like 1 (*RP1L1*, OMIM 608581) is the only confirmed gene associated with OMD.[5] It is mapped to human chromosome 8p and spans 50 kb of genomic DNA; it is composed of four exons, but exon 1 is noncoding.[6] Immunohistochemical analysis revealed that this gene is expressed in the retinal rod and cone photoreceptors of cynomolgus monkeys.[5] Some studies found that *RP1L1* appeared to be involved in maintenance of the morphology and function of photoreceptors.[7–9] To date, the Human Gene Mutation Database (HGMD) has recorded 24 variants of *RP1L1* related to OMD. Of the 24 variants, c.133C>T (p.R45W) is the most common variant and is found in all populations, indicating a mutation hotspot.[4,10,11] In addi-

tion, there is another mutation hotspot that includes six amino acids (1196–1201) downstream of the doublecortin (DCX) domain.[12] Other phenotypes associated with *RP1L1* mutations are autosomal recessive retinitis pigmentosa, autosomal recessive cone dystrophy, and possibly a digenic form of syndromic retinal dystrophy.[10,13,14]

To date, numerous studies describing OMD patients with *RP1L1* mutations have been reported, but limited data are available for the Chinese population.[4,15,16] Thus, this study aims to investigate the clinical and genetic characteristics of a small cohort of Chinese OMD patients.

Methods

Subjects

A total of 15 Chinese patients with OMD were included in this study between 2016 and 2019. The study was performed in compliance with the tenets of the Declaration of Helsinki and approved by the Ethics Committee of the Eye and ENT Hospital of Fudan University. An informed consent form was obtained from all the subjects or their guardians. The clinical diagnostic criteria for OMD were as follows: (1) progressive decrease in central vision with normal appearing fundus and normal ffERG results, and (2) reduced foveal mfERG amplitudes. Patients with a clinical diagnosis of OMD or harboring a heterozygous pathogenic *RP1L1* variant were included.

Clinical Evaluations

Nine probands underwent detailed clinical evaluations, including evaluations of medical history and family history and complete ophthalmic examinations. Chief complaints, onset of disease, and duration of disease were recorded in detail. The ophthalmic examinations included determination of best-corrected visual acuity (BCVA) in decimal units; color vision examination (Ishihara color plate test); slit-lamp examination; dilated fundus examination and photography; SD-OCT and fundus autofluorescence (FAF; Spectralis HRA+OCT, Heidelberg Engineering, Inc., Heidelberg, Germany); ffERG and mfERG (VERIS Science 6.0; Electro-Diagnostic Imaging, Inc., Redwood City, CA, USA; according to the standards of the International Society for Clinical Electrophysiology of Vision); and Humphrey perimetry (Carl Zeiss Meditec, Inc., Dublin, CA, USA).

Genetic Analysis

Peripheral blood samples were collected from the nine probands and their family members. Genomic DNA was extracted from blood with the Qiagen FlexiGene DNA Kit (Hilden, Germany) according to standard procedures. The capture panel was custom designed and produced by the Beijing Genomics Institute (Shenzhen, China) for this study. It contained the exon sequences of 792 genes (Supplementary Table S1), as well as 30 bp from either side of the exonic region. Enriched libraries were sequenced with the Illumina Hiseq 2000 platform (Illumina, Inc., San Diego, CA, USA). Reads were aligned to the hg38 human reference sequence using the Burrows–Wheeler Aligner, version 0.7.10 (BWA-MEM).

The following four databases were used for annotation to eliminate the benign variants with minor allele frequency > 0.1%: 1000 Genomes Project (http://browser.1000genomes.org/), dbSNP (http://www.ncbi.nlm.nih.gov/projects/SNP), ESP6500 (http://evs.gs.washington.edu/EVS/), and ExAC (http://exac.broadinstitute.org). All identified variants were analyzed using four online prediction tools: MutationTaster (http://www. mutationtaster.org/), Sorting Intolerant from Tolerant (https://www.sift.co.uk/), FATHMM (http://fathmm.biocompute.org.uk/), and Polymorphism Phenotyping v2 (http://genetics.bwh.harvard.edu/pph2/). Previously reported variants were determined according to ClinVar (https://www.ncbi.nlm.nih.gov/clinvar/) and HGMD Professional version 2019.2 (http://www.hgmd.cf.ac.uk/ac/index.php). We combined total coverage depth, quality score, potential deleterious effects, and mutation reports in HGMD, ClinVar, and Online Mendelian Inheritance in Man to perform variant prioritization. Finally, Sanger sequencing and cosegregation analyses were performed within family members to verify the candidate variants. The cDNA NM_178857.5 and protein NP_849188.4 sequences were used for *RP1L1* mutation nomenclature. For DNA numbering, +1 corresponded to the A of the ATG translation initiation codon. Variants were classified according to the American College of Medical Genetics and Genomics guidelines.

Data Analysis

All images were evaluated independently by two authors (DW and FG), who were blinded to the BCVA and symptom duration information. If there was any disagreement between the two authors, it was resolved by a senior retinal specialist (GX). The thickness of the foveal outer nuclear layer (ONL), between the internal limiting membrane (ILM) and the external limiting membrane (ELM) at the center of the fovea; the thickness of the foveal photoreceptor, between the inner borders of the ELM and the retinal pigment epithelium (RPE) at the center of the fovea; and the thickness of the central fovea, from the ILM to the RPE at the center of the fovea, were measured manually using the digital caliper tool in the Spectralis OCT system (Heidelberg Engineering). All statistical analyses were performed using SPSS Statistics 20.0 (IBM, Armonk, NY, USA). Correlation parameters were calculated using Pearson analysis; $P < 0.05$ was considered the threshold of statistical significance.

Results

Demographics

The pedigree charts and genetic characteristics of the nine families are shown in Figure 1. Of the 15 patients with OMD, the clinical characteristics of nine probands (Table) were analyzed. Some data obtained from patient 7 have been published elsewhere.[17] There were six affected males (66.7%) and three affected females (33.3%). The median age was 27.0 years (range, 14–55 years). Autosomal dominant family history was clearly reported in five probands (55.6%), whereas three probands were sporadic (33.3%). One proband had no family history, and genetic testing confirmed a de novo mutation (11.1%) (Fig. 2).

Clinical Findings

The age at onset varied widely from 6 to 51 years, and the median age of onset was 25.0 years. Among the probands, one presented with decreased central vision before the age of 10 years. All probands had reduced visual acuity, and

Investigative Ophthalmology & Visual Science

Table. Clinical and Genetic Characteristics of Patients with OMD in This Study

Patient	1	2	3	4	5	6	7	8	9
Sex	M	M	F	M	M	M	M	F	F
Age (y)	14	27	39	18	16	15	38	55	48
Age at onset (y)	12	25	37	15	6	12	28	51	44
Inheritance	Sporadic	Sporadic	AD	AD	AD	de novo	AD	Sporadic	AD
BCVA	0.3/0.3	0.4/0.5	0.4/0.05	0.15/0.2	0.1/0.1	0.2/0.25	0.5/0.5	0.05/0.04	0.09/0.1
Photophobia	–	+	+	–	–	+	–	+	+
Color vision	Red-green deficiency	–	–	Red-green deficiency	Red-green deficiency	–	–	Red-green deficiency	Red-green deficiency
Central scotoma	+	–	+	+	+	+	–	+	+
Thickness of outer nuclear layer (μm)	84/96	101/96	119/117	103/111	98/98	88/101	70/90	74/80	80/83
Thickness of photoreceptor (μm)	62/62	60/73	70/61	60/62	65/59	70/70	65/70	61/63	57/62
Thickness of central fovea (μm)	177/183	181/188	207/203	197/196	176/181	179/182	158/172	196/192	168/173
Nucleotide change	c.133C>T	c.133C>T	c.133C>T	c.133C>T	c.133C>T	c.133C>T	c.133C>T	c.133C>T	c.3596C>G
Amino acid change	p.R45W	p.R45W	p.R45W	p.R45W	p.R45W	p.R45W	p.R45W	p.R45W	p.S1199C
Exon	Exon2	Exon2	Exon2	Exon2	Exon2	Exon2	Exon2	Exon2	Exon4

M, male; F, female; AD, autosomal dominant.

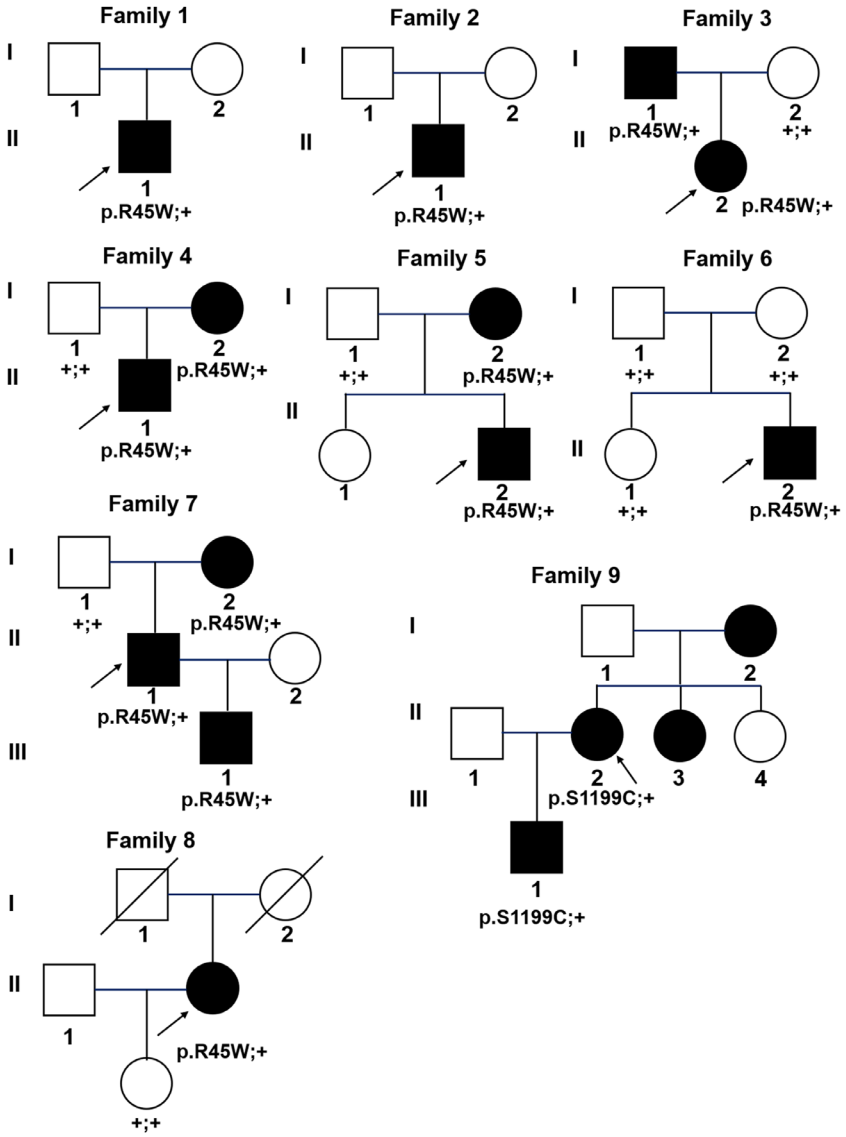

Figure 1. Pedigrees of nine Chinese families with OMD. Squares represent males; circles, females; empty symbols, normal controls; and filled symbols, affected patients. The probands are marked by an arrow.

five probands complained of photophobia (5/9, 55.6%). Red-green deficiency was detected in five probands (5/9, 55.6%). Seven probands had a central scotoma (7/9, 77.8%). The median decimal BCVA was 0.20, with a range of 0.04 to 0.5. Asymmetrical visual decline occurred in one proband with visual acuity of 0.4 and 0.05 (1/9, 11.1%). There was no significant correlation between decimal BCVA and age of onset ($P = 0.407$) or symptom duration ($P = 0.783$).

All probands showed reduced foveal amplitudes by mfERG, indicating localized macular dysfunction. The classical morphological changes observed by SD-OCT were the absence of an IZ and blurring of the EZ of photoreceptors at the macula, observed in all probands. In addition, disruption of the ELM was noted in one proband (1/9, 11.1%) (Fig. 3A). None of the probands exhibited abnormal findings in the RPE layer by SD-OCT. All probands presented with foveal thinning, and the mean central retinal thickness was 183.8 ± 12.8 µm; however, decimal BCVA was not significantly related to foveal thickness ($P = 0.284$). The mean thicknesses of the foveal ONL and the foveal photoreceptor were 93.8 ± 13.9 µm and 64.0 ± 4.7 µm, respectively. A significant correlation was found between decimal BCVA and the thickness of the foveal photoreceptor ($r = 0.591$; $P = 0.01$) (Fig. 4), whereas decimal BCVA was not correlated with foveal ONL thickness ($P = 0.885$). The fundus near-infrared (NIR) reflectance was determined in all probands, and the central round lesions with low NIR reflectance was detected in 12 eyes (12/18, 66.7%). These areas corresponded to the abnormal IZ and EZ on SD-OCT (Fig. 3B). The AF images showed ring-like faint hyperfluorescence around the macula in four eyes (4/18, 22.2%) (Fig. 3D).

Genetic Findings

Two known heterozygous pathogenic variants of *RP1L1* were identified in the small cohort of Chinese OMD patients: p.R45W (8/9 families, 88.9%) and p.S1199C (1/9 families, 11.1%). To date, 26 variants have been identified in the 196

Investigative Ophthalmology & Visual Science

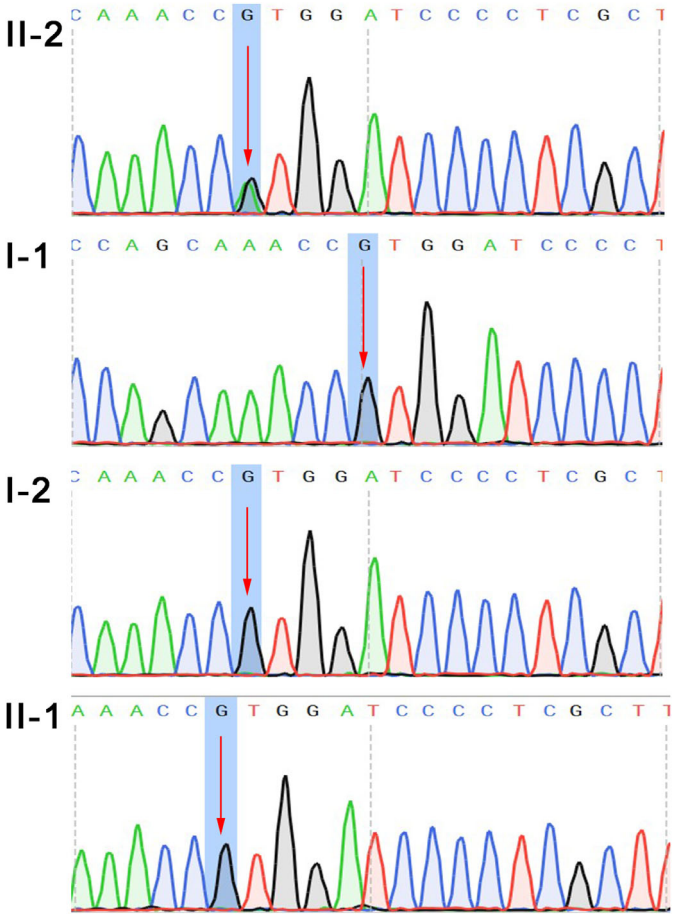

Figure 2. Sanger sequencing. Sanger sequencing results of the *RP1L1* variant in family 6. The arrow indicates the position of the variant.

individuals from 101 unrelated families, including the data in this study (Supplementary Table S2). Of the 26 variants, 92.3% (n = 24) were missense mutations, and frameshift and nonsense mutations accounted for 3.8% (n = 1 each). The most frequent variant was p.R45W (71/101 families, 70.3%), followed by p.S1199C (7/101 families, 6.9%), located within two previously reported mutation hotspots.[4] A schematic diagram showing the location of all previously reported *RP1L1* variants is presented in Figure 5. Five of the 26 variants (19.2%) were located in two DCX domains (residues 33–133 and 147–228), and these domains in combination with the RP1 domain appeared to be necessary for localization of *RP1L1* to the outer segment axoneme of photoreceptors.[7,11,18] No variant was found in the RP1 domain (residues 307–340) of the RP1L1 protein. In addition, variants were clustered in two regions (residues 950–960 and 1196–1201), the latter being a mutation hotspot, as previously reported.[12]

Discussion

In this study, we reviewed the clinical and genetic characteristics of a small Chinese cohort with OMD in detail and identified two known *RP1L1* variants, which are the two most common variants in the East Asian population. The allele frequencies of the variant p.R45W in East Asian, South Asian, and European (non-Finnish) populations are 0.0001167, 0.000000, and 0.00003046, respectively. The variant p.S1199C is not found in the ExAC or 1000 Genomes Project database, but all 12 reported patients harboring this variant were East Asian.[4,19,20] This indicated that these two variants were more common in the East Asian population than in other populations. Previous studies showed that the penetrance of the variant p.R45W was incomplete, ranging from 38% to 85%.[5,10,11] In contrast, the variant p.S1199C has never been reported in healthy individuals. In this cohort, all genetically affected patients presented with ocular abnormalities. The identification of healthy carriers is vital for determining a penetrance; however, it is unusual for asymptomatic individuals to visit clinics or hospitals. Therefore, carrier screening is helpful, and detailed clinical assessments and long-term, regular follow-up might be considered for asymptomatic individuals affected genetically.

The IZ absence and EZ blurring of photoreceptor microstructures observed by SD-OCT are classical changes in OMD patients and were observed in all probands of our cohort. However, Kato et al.[20] found that central foveal microstructures could be spared in some patients carrying pathogenic *RP1L1* variants; the visual acuity of these patients was generally well preserved, and mfERG results could even be normal, but SD-OCT revealed abnormal microstructures in the parafoveal regions. This finding demonstrated that SD-OCT is more sensitive in detecting pathologic changes of OMD than other examination methods and contributes to the improvement of early diagnostics. In addition, SD-OCT is useful for monitoring the progression of OMD. Consistent

Investigative Ophthalmology & Visual Science

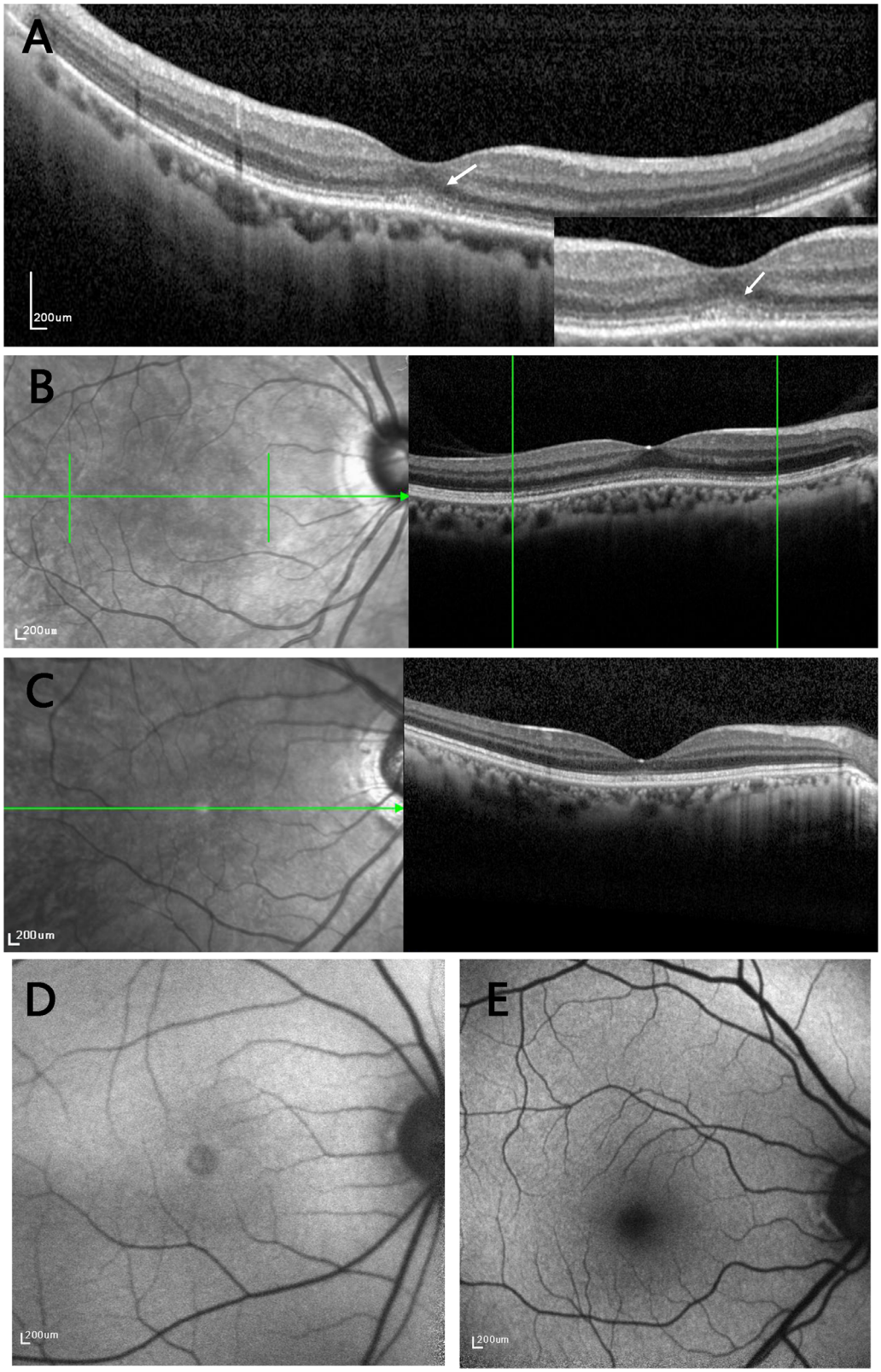

Figure 3. Multimodal images in the probands with OMD. (A) Focal disruption of the ELM (arrow). (B) Fundus near-infrared (NIR) reflectance showed the central round lesions with low NIR reflectance, corresponding to the abnormal IZ and EZ on SD-OCT. (C) A normal infrared reflectance image. (D) The AF image revealed ring-like faint hyperfluorescence around the macula. (E) A normal AF image.

Investigative Ophthalmology & Visual Science

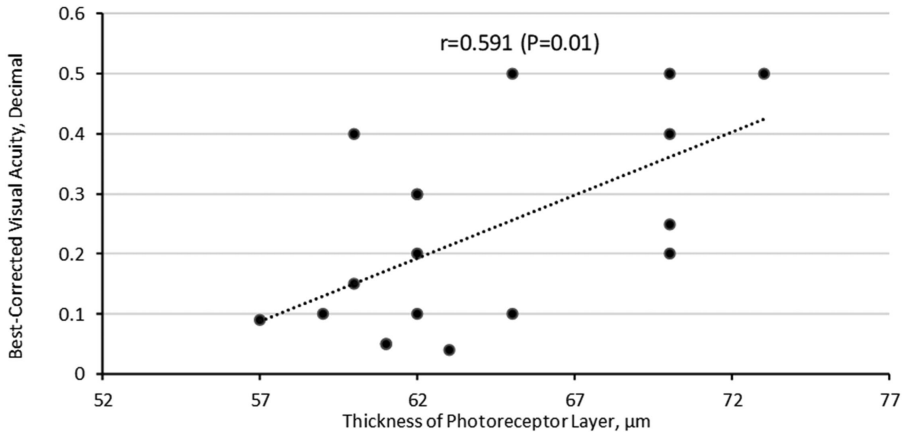

Figure 4. Correlation of BCVA with the thickness of photoreceptors.

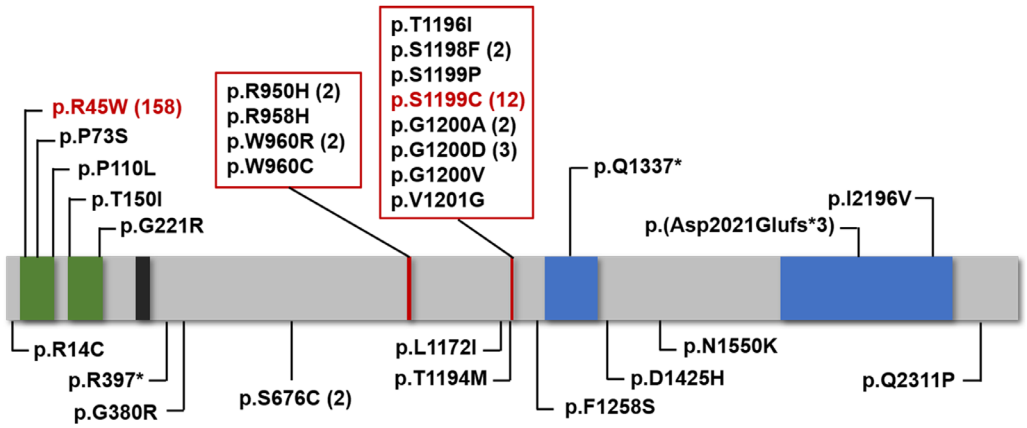

Figure 5. Schematic representation of the *RP1L1* gene, all known variants related to OMD, and their frequencies. Two DCX domains (residues 33–133 and 147–228) are labeled in green, the RP1 domain (residues 307–340) is labeled in black, two repeat regions of the C-terminal (residues 1278–1402 and 1836–2244) are labeled in blue, and two clustered regions of variants (residues 950–960 and 1196–1201) are labeled in red.

with previous research,[3] we found that foveal photoreceptor thickness was related to visual acuity, whereas foveal thickness and ONL thickness were not significantly associated with visual acuity, even though thinning was observed in all probands.

Upon fundus NIR reflectance imaging, disrupted photoreceptor microstructures showed lower NIR reflectance than the surrounding fundus reflex, which was observed in 12 of 18 eyes (66.7%). Similarly, the proportion was 78%, as reported in a previous study.[3] NIR reflectance at the fundus is mainly affected by absorption and reflection; therefore, this finding indicates that photoreceptors are important reflectors of NIR light and further supports the value of NIR reflectance imaging for OMD diagnosis. In addition, only four eyes (4/18, 22.2%) presented with parafoveal ring-like faint hyperfluorescence on AF in this cohort, consistent with the results of previous studies.[3,21] Possible reasons for apparent hyperautofluorescence include a window defect due to decreased absorption of light by photoreceptor outer segments or macular luteal pigment or a real increase in AF due to the accumulation of a fluorophore; alternatively, relative hyperautofluorescence may be apparent due to an adjacent zone of hypoautofluorescence. Notably, the RPE layer, as the main source of AF, was intact in all probands with OMD; therefore, multimodal imaging is necessary for OMD patients. This approach can greatly aid physicians in diagnosing and monitoring disease progression and is valuable for understanding the pathologic characteristics of OMD.

In addition to the above structural parameters, visual acuity is a highly significant functional parameter for monitoring the severity or progression of OMD. In this cohort, visual acuity varied widely from 0.04 to 0.5; however, no significant correlation was found between visual acuity and onset and duration, unlike the results of previous studies.[4,8] This may be related to the small number of patients included in this study. Another limitation of our study is that it is a cross-sectional retrospective study, and more accurate data regarding disease progression could not be obtained. Therefore, in the future, longitudinal large-cohort studies will be essential for understanding the natural course and structure–function relationship of OMD.

In conclusion, two known *RP1L1* variants were identified (p.R45W and p.S1199C) in this study, further confirming that these two variants are common in East Asian populations and have higher frequencies in East Asian populations than

Investigative Ophthalmology & Visual Science

in other populations. In addition, we found that foveal photoreceptor thickness was associated with visual acuity, which is helpful for monitoring progression. Finally, multimodal imaging and genetic testing are recommended for early diagnosis and accurate evaluation in individuals with suspected OMD.

Acknowledgments

Supported by the National Natural Science Foundation of China (Nos. 81770925 and 81790641) and by the Non-Profit Central Research Institute Fund of Chinese Academy of Medical Sciences (2018PT32019).

Disclosure: **D.-D. Wang**, None; **F.-J. Gao**, None; **J.-K. Li**, None; **F. Chen**, None; **F.-Y. Hu**, None; **G.-Z. Xu**, None; **J.-G. Zhang**, None; **H.-X. Sun,** None; **S.-H. Zhang**, None; **P. Xu**, None; **G.-H. Tian,** None; **J.-H. Wu**, None

References

1. Miyake Y, Ichikawa K, Shiose Y, Kawase Y. Hereditary macular dystrophy without visible fundus abnormality. *Am J Ophthalmol*. 1989;108:292–299.
2. Fujii S, Escano MF, Ishibashi K, Matsuo H, Yamamoto M. Multifocal electroretinography in patients with occult macular dystrophy. *Br J Ophthalmol*. 1999;83:879–880.
3. Ahn SJ, Ahn J, Park KH, Woo SJ. Multimodal imaging of occult macular dystrophy. *JAMA Ophthalmol*. 2013;131:880–890.
4. Fujinami K, Yang L, Joo K, et al. Clinical and genetic characteristics of East Asian patients with occult macular dystrophy (Miyake disease); EAOMD Report No.1. *Ophthalmology*. 2019;26:1432–1444.
5. Akahori M, Tsunoda K, Miyake Y, et al. Dominant mutations in RP1L1 are responsible for occult macular dystrophy. *Am J Hum Genet*. 2010;87:424–429.
6. Bowne SJ, Daiger SP, Malone KA, et al. Characterization of RP1L1, a highly polymorphic paralog of the retinitis pigmentosa 1 (RP1) gene. *Mol Vis*. 2003;9:129–137.
7. Yamashita T, Liu J, Gao J, et al. Essential and synergistic roles of RP1 and RP1L1 in rod photoreceptor axoneme and retinitis pigmentosa. *J Neurosci*. 2009;29:9748–9760.
8. Miyake Y, Tsunoda K. Occult macular dystrophy. *Jpn J Ophthalmol*. 2015;59:71–80.
9. Conte I, Lestingi M, den Hollander A, et al. Identification and characterisation of the retinitis pigmentosa 1-like1 gene (RP1L1): a novel candidate for retinal degenerations. *Eur J Hum Genet*. 2003;11:155–162.
10. Zobor D, Zobor G, Hipp S, et al. Phenotype variations caused by mutations in the RP1L1 gene in a large mainly German cohort. *Invest Ophthalmol Vis Sci*. 2018;59:3041–3052.
11. Davidson AE, Sergouniotis PI, Mackay DS, et al. RP1L1 variants are associated with a spectrum of inherited retinal diseases including retinitis pigmentosa and occult macular dystrophy. *Hum Mutat*. 2013;34:506–514.
12. Fujinami K, Kameya S, Kikuchi S, et al. Novel RP1L1 variants and genotype-photoreceptor microstructural phenotype associations in cohort of Japanese patients with occult macular dystrophy. *Invest Ophthalmol Vis Sci*. 2016;57:4837–4846.
13. Kikuchi S, Kameya S, Gocho K, et al. Cone dystrophy in patient with homozygous RP1L1 mutation. *Biomed Res Int*. 2015;2015:545243.
14. Liu YP, Bosch DG, Siemiatkowska AM, et al. Putative digenic inheritance of heterozygous RP1L1 and C2orf71 null mutations in syndromic retinal dystrophy. *Ophthalmic Genet*. 2017;38:127–132.
15. Agange N, Sarraf D. Occult macular dystrophy with mutations in the RP1L1 and KCNV2 genes. *Retin Cases Brief Rep*. 2017;11(suppl 1):S65–S67.
16. Fu Y, Chen KJ, Lai CC, Wu WC, Wang NK. Clinical features in a case of occult macular dystrophy with RP1L1 mutation. *Retin Cases Brief Rep*. 2019;13:158–161.
17. Qi YH, Gao FJ, Hu FY, et al. Next-generation sequencing-aided rapid molecular diagnosis of occult macular dystrophy in a Chinese family. *Front Genet*. 2017;8:107.
18. Coquelle FM, Levy T, Bergmann S, et al. Common and divergent roles for members of the mouse DCX superfamily. *Cell Cycle*. 2006;5:976–983.
19. Kabuto T, Takahashi H, Goto-Fukuura Y, et al. A new mutation in the *RP1L1* gene in a patient with occult macular dystrophy associated with a depolarizing pattern of focal macular electroretinograms. *Mol Vis*. 2012;18:1031–1039.
20. Kato Y, Hanazono G, Fujinami K, et al. Parafoveal photoreceptor abnormalities in asymptomatic patients with RP1L1 mutations in families with occult macular dystrophy. *Invest Ophthalmol Vis Sci*. 2017;58:6020–6029.
21. Fujinami K, Tsunoda K, Hanazono G, et al. Fundus autofluorescence in autosomal dominant occult macular dystrophy. *Arch Ophthalmol*. 2011;129:597–602.